Staring observations of compact sources at 3.6μm with ISOPHOT

Ágnes Kóspál, Péter Ábrahám, Attila Moór

Konkoly Observatory, Budapest, Hungary
27-October-2005

Version 1.0

Contents

1 Introduction

At Konkoly Observatory we work on a long-term project aiming at the re-calibration of selected ISOPHOT observing modes. The improved results are presented in the forms of photometric catalogues and spectral atlases, and are available in the ISO Data Archive as *Highly Processed Data Products (HPDPs)*. In the present document we (1) report on the re-calibration of staring observations of compact sources measured at 3.6μm with ISOPHOT, (2) present the photometric accuracy achieved, and (3) describe the photometric catalogue created.

2 Description of the observing mode

2.1 Observing sequence

Staring observations with the P1 detector could be performed using the PHT03 (multi-filter photometry), PHT04 (multi-aperture photometry), PHT05 (absolute photometry), PHT17/18/19 (sparse map) and PHT99 (mode reserved for calibrators) Astronomical Observing Templates. These staring sequences typically consist of a pair of ON and OFF positions. However, a special feature of the P1_3.6 micrometer observations is that the zodiacal background signal was negligible in all but the largest apertures. Thus in point source observations taken with the usual $23''$ or $52''$ apertures background subtraction was not absolutely necessary, and many observers have really skipped the OFF-observation (this was not a good strategy, however, if the background was not purely zodiacal light, e.g. when the OFF-position was towards a bright reflection nebula).

2.2 P1_3.6 observations in the Legacy Archive

We searched the archive for 3.6μm observations, limiting the query to the mentioned AOTs. The search resulted in 629 measurements carried out by the P1 detector. Cross-checking them one-by-one with the SIMBAD database we identified and selected those which are presumably compact sources.

The complete processing scheme of P1 staring observations in the ISO Pipeline is documented in the ISO Handbook. We emphasize that for the photometric calibration the software used the actual responsivity derived from the corresponding FCS observation. In the following we will point out that default responsivity works better for P1_3.6 data.

According to the ISOPHOT Handbook Sect. 9.2, the absolute accuracy of the P1 detector on point sources in staring mode is better than 10% for bright sources in the range of 50 - 6000 Jy, while about 40% for intermediate faint sources of 0.1 - 50 Jy.

3 Recalibration of P1_3.6 observations of compact sources

3.1 Recalibration strategy

The calibration strategy was the same we utilised in other observing modes: first we identify those measurements from the Archive in the selected observing mode which can potentially be used as secondary standard observation (usually normal star measurements), then we compare their predicted and measured fluxes. If systematic deviations or large scatter are experienced, we develope new correction algorithms (for details on calibration strategy see Moór et al. 2003).

3.2 Collection of "secondary standards" from the archive

Among the P1_3.6 observations collected from the Archive we identified 44 measurements on 40 normal stars which can be possibly used as secondary standards. In addition, since the normal stars failed to cover the low flux range (<500 mJy), we collected 7 observations of young stellar objects where L-band magnitudes from the ground were available.

3.3 Flux prediction for the secondary standards

The fluxes of the normal stars at $3.6\,\mu$m were predicted as follows. The ISOPHOT photometric system was defined by the photospheric templates/models of $\sim$ 160 stars produced by M. Cohen and P. Hammersley (hereafter we refer them as primary standards). Since Cohen & Hammersley models are not available for most of the secondary standards, we evaluated the primary standards, and determined a relationship between their $K - [3.6]$ magnitude

differences and $(B-V)$ colours. The relationship is shown in Figure 1. A fourth-order polynomial appropriately fits the relation. The precision of the predicted fluxes is $\sim 3\%$.

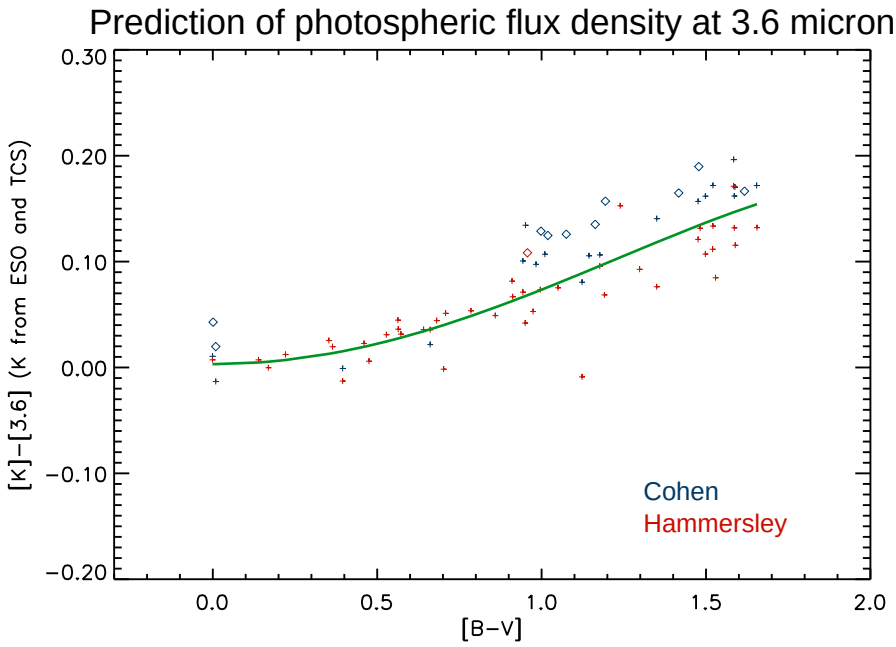

Figure 1: Relationship between the $K-[3.6]$ magnitude differences and $(B-V)$ colours derived from the ~ 160 stellar templates provided by M. Cohen and P. Hammersley to ISO.

For secondary standards (normal stars) we collected the Johnson B and V magnitudes mainly from the Hipparcos catalogue, and K magnitude from the 2MASS survey. Their 3.6μm fluxes were predicted from the $K-[3.6] vs. (B-V)$ relation, assuming a zero-magnitude flux of 266 Jy (the flux prediction is implemented in an IDL procedure). Note that this method is valid only for stars without infrared excess i.e. where we observe the photospheric irradiation only. This cannot be guaranteed for any particular star in advance, but we assume that the majority of the normal stars do not have any infrared excess.

For the young stellar objects we check the Catalog of Infrared Observations (Gezari et al., available via the VIZIER service), and converted the L-band or L$'$ band magnitudes to flux.

3.4 Processing the secondary standards

The data processing was performed with PIA 10.0. At the SRD level the observations were visually checked for signal transients and the drifting part of the measurement was manually discarded. The flux calibration was performed with both the default and actual responsivities, and all the later analyses were performed parallel with both responsivities.

3.5 Background subtraction

Unfortunately, a lot of source measurements have no OFF measurement. Although the sky background is expected to be low at 3.6 μm, the OFF-measurements might still show an offset due to effects of the detector or the readout electronics. We collected from the archive a number of empty-sky observations (background fields near point sources). We derived an average background value of 39 ± 9 mJy, which was calculated by the averaging of all the available (31) OFF measurements (see Fig. 2). No dependence of the off-signal on the aperture area could be seen,

proving our pre-assumption that the signal is related to the detector rather than to the phyisical background (in this case the zodiacal light). In the following this average value was subtracted from those ON-source observations which were not accompanied with OFF-source measurement.

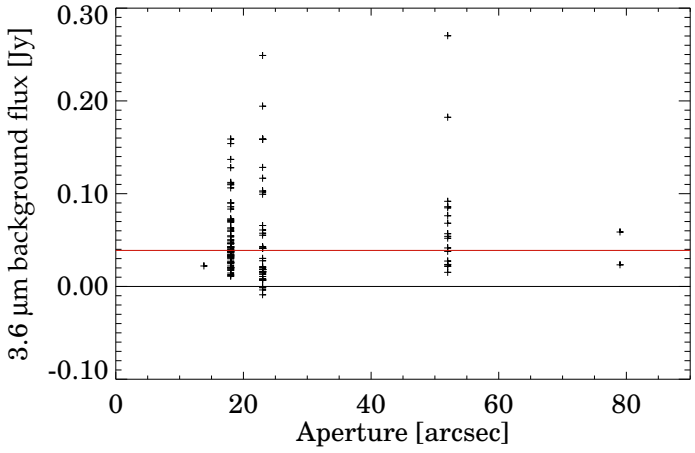

Figure 2: Offset = 39 +/- 9 mJy

4 Comparison of measured and predicted fluxes

Then we compared the predicted and measured fluxes of the 40 secondary standards and 7 young stellar objects. The result is shown in Figure 3 (black dots). The plotted values are all photometric values obtained with default responsivity: the corresponding values with the actual responsivity showed a significantly higher scatter, thus we concluded that default response is the right choice for the P1 detector.

We fitted the distribution with a curve which will be used as an empirical correction curve to cancel systematic deviations from the predicted fluxes. The form the the curve is the following:

for faint fluxes ($F < 0.4$ Jy):

$$F_{\rm predicted} = 0.0132 + 1.170 \times F_{\rm measured} \tag{1}$$

for fluxes $0.4 < F < 0.8$ Jy):

$$F_{\rm predicted} = 0.8160 \times F_{\rm measured}^{0.5760} \tag{2}$$

for fluxes $0.8 < F < 10$ Jy):

$$F_{\rm predicted} = 0.9225 \times F_{\rm measured}^{1.1256} \tag{3}$$

The offset value in Eq. 1 is of low significance, but it might be a physical effect caused by a small overshoot phemonenon often observed in very faint P1 measurements at the beginning of the data stream. The fitted curve as well as the original measurements are presented in Fig. 4.

4.1 Error budget

A photometric accuracy value representative of the whole ensemble can be derived from the dispersion around the fitted line. This way we determined σ=56 mJy at low level and σ=10.8% at high flux level. These values are significantly better then those claimed in the Handbook for this observing mode. The improvement is partly related to the adoption of default responsivity, and partly to our newly developed empirical correction formula.

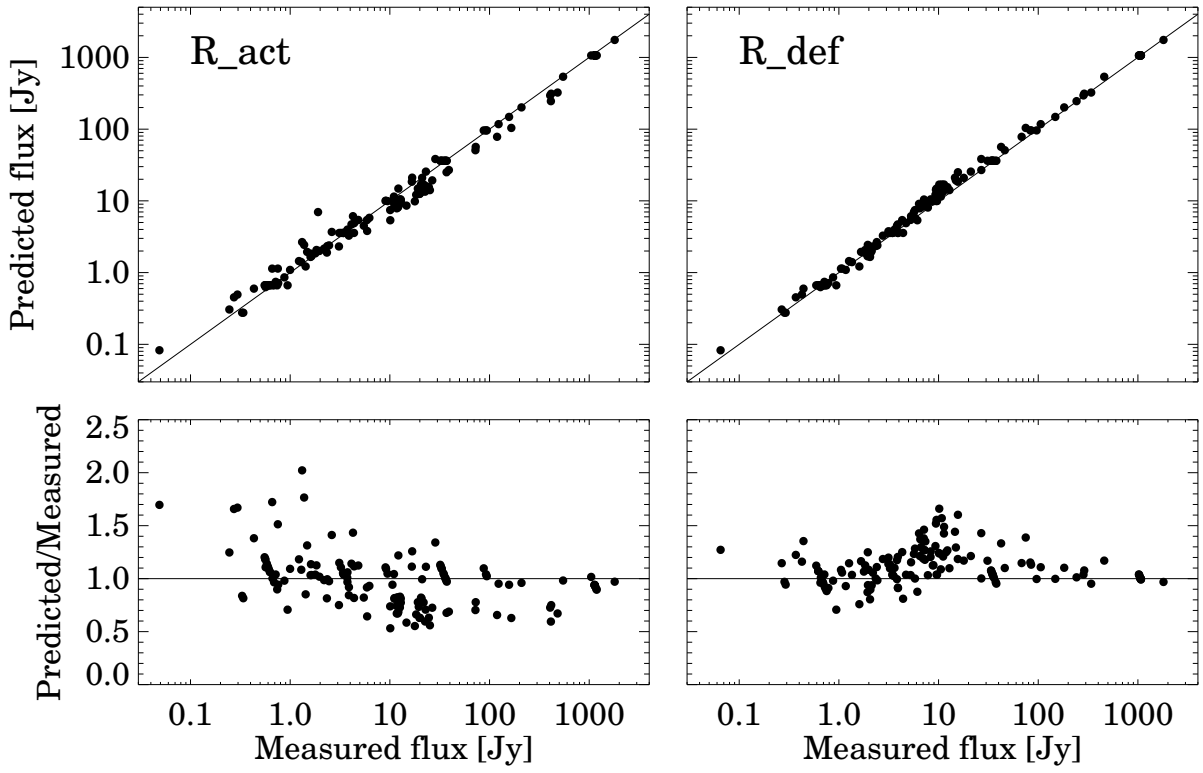

Figure 3: Relationship between the $K - [3.6]$ magnitude differences and $(B - V)$ colours derived from the ~ 160 stellar templates proveded by M. Cohen and P. Hammersley to ISO.

4.2 Implementation of the correction formula

The empirical photometric correction curve of Fig. 4 was represented as an array of values interpolated for a fine grid, and the array as well as the grid were stored in an IDL save file. We wrote an IDL function which perfoms the empirical correction on the basis of the save file. Note that since the default responsivity of the P1 detector is practically constant in time, our flux dependent correction curve – determined at the flux density level – could in principle be transformed to a correction at signal level (in V/s), and could this way be merged with the signal linearization.

The final photometric uncertainties were computed as the maximum of the error bar provided by PIA and the average error value representative of the whole ensemble.

4.3 Is there any physics behind the correction formula?

It is well known that the general shape of the P1 transient curve starts with a relatively high initial jump (which may even have the form of a small overshoot), then continues with an increasing part reaching a peak, and finally there is a slow decrease after the peak. The correction curve we derived qualitatively agrees with the described shape of the transient curve, so we speculate that the physical reason behind the need for photometric correction is that the different observations are affected by different parts of the transient curve depending on the flux level and on the measurement time.

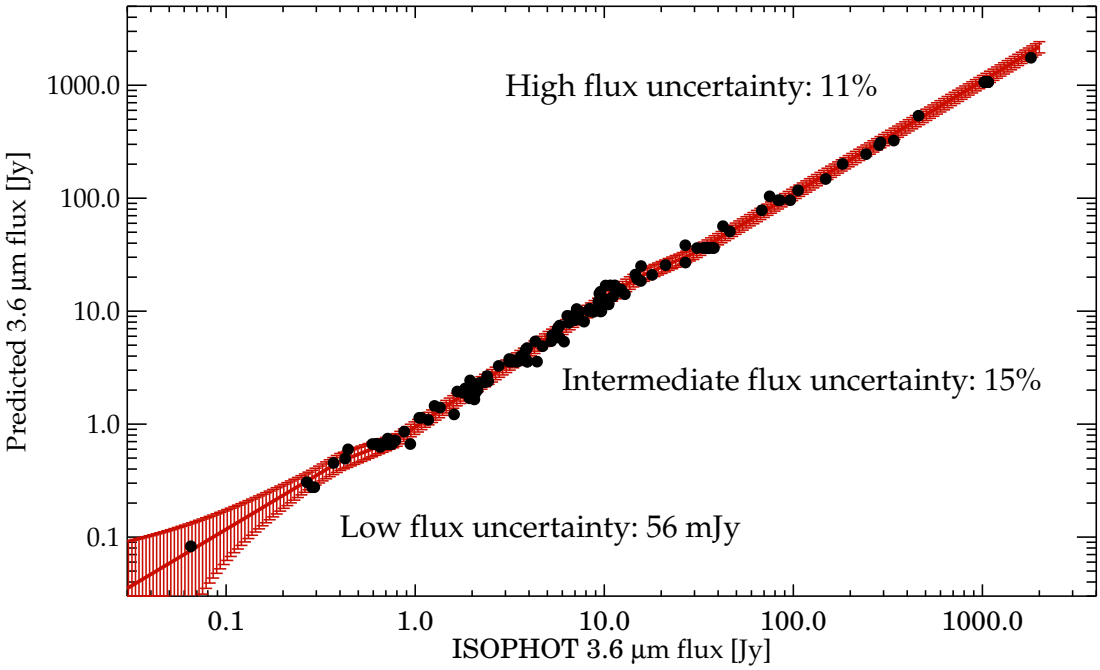

Figure 4: Comparison of measured and predicted fluxes ar 3.6 micron. Measurements obtained by P1 detector in PHT03 and PHT04 modes.

5 Conclusions and outlook

From our study it became clear that the photometric accuracy of the P1 3.6μm staring observations is higher than the general accuracy values of the P1 detector claimed in the ISOPHOT Handbook. Adopting always default responsivities, and applying an empirical photometric correction we were able to achieve 56 mJy at faint level and about 11% at high flux level.

The scatter of points around the fitted curve in Fig. 4 can be still partly systematic, e.g. related to the length of the measurement, to the reset interval used, or to the signal level of the preceeding P1 observation within the same TDTNUM. Further analyses, involving also stars from the AOTs PHT05 and PHT99, may still refine the picture and lower further the measurement uncertainty.

References

Moór A., Ábrahám P., Csizmadia Sz., Kiss Cs.,2003, *A catalogue of ISOPHOT far-infrared observations of normal stars in mini-map mode*

6 Appendix: Description of the Catalogue

After developing the empirical photometric correction formula and validating the calibration on the secondary standards, we process all P1_3.6 compact source observations (in total 291) and compiled a photometric catalogue. Details of the processing are identical with the processing of the secondary standards. In the following we describe the fields of the catalogue (the catalogue is available only electronically).

Column	Field	Unit	Format	Description
(1)	Object name			SIMBAD compatible name. Filled if a compact source from SIMBAD can be associated with the ISOPHOT target without doubt. Note that asteroids have no SIMBAD compatible name.
(2)	Object type			Standard SIMBAD code for object type
(3)	ISO name			Object name given by the ISO observer
(4)	TDTNUM_ON			The 8-digit TDTNUM of the on-source observation
(5)	On_ Meas.			Index of the on-source measurement within TDTNUM_ ON
(6)	RA(2000)			Right ascension of the ISO position [h,m,s]
(7)	Dec(2000)			Declination of the ISO position [d,m,s]
(8)	Detector			ISOPHOT detector (P1, P2, P3, C100, or C200)
(9)	Wavelength	[micron]		Nominal wavelength of the ISOPHOT filter
(10)	Aperture	[arcsec]		Circular for P1,P2,P3, square for C100 and C200 detectors
(11)	Epoch			Epoch of the observation
(12)	TDTNUM_ OFF			The 8-digit TDTNUM of the off-source observation
(13)	Off_Meas.			Index of the off-source measurement within TDTNUM_OFF
(14)	Flux density	[Jy]		Flux density of the source. No colour correction applied
(15)	Flux uncertainty	[Jy]		Flux uncertainty. No colour correction applied.
(16)	Object size			Indicates if the object is point-like (P) or extended (E)
(17)	Quality			Quality of the observation R1 – Standard processing according to the scheme described in the report.

Table 1: Description of the catalogue